

Probabilistic Assessment of Service Life of Failure Risk

N. R. Moore and D. H. Ebbeler
Jet Propulsion Laboratory, California Institute of Technology, Pasadena, CA 91109
Telephone: (818) 354-4926

M. Creager
Structural Integrity Engineering, Chatsworth, CA

ABSTRACT: A probabilistic methodology for evaluating failure risk, assessing service life, and establishing design parameters for elements of mechanical, electro-optical, or electronic system has been developed. In this methodology, analytical modelling based on the physics or mechanics of failure phenomena is combined with experience from tests and service to quantify failure risk. The methodology is particularly valuable when information on which to base design analysis or failure prediction is sparse, uncertain, or approximate and is expensive or difficult to acquire. Sensitivity analyses conducted as a part of the probabilistic methodology can be used to evaluate alternative measures to control risk, such as design changes, testing, or inspections, thereby enabling limited program resources to be allocated more effectively. Examples of failure phenomena to which this methodology is applicable include fatigue crack initiation, fatigue crack growth, erosion, radiation damage, and wear. The probabilistic methodology and an example application to fatigue crack growth in a heat exchanger tube are presented.

INTRODUCTION

The assessment and management of the risk of failure to meet service life, performance, or reliability goals can be improved by using a risk assessment approach that can incorporate information quantitatively from both experience and analytical modeling. In the probabilistic failure risk assessment approach presented here, experience and analytical modeling are used in a statistical structure in which uncertainties about failure prediction are quantitatively treated. Such probabilistic analysis can be performed with the information available at any time during the design, development, verification, or service of mechanical or electronic systems to obtain a quantitative estimate of failure risk that is warranted by what is known about a failure mode. This probabilistic method is applicable to failure modes which can be described by analytical models of the failure phenomena, even when such models are uncertain or approximate.

By conducting risk sensitivity analyses probabilistically for selected failure modes, sources of unacceptable failure risk can be identified and corrective action can be delineated. Design revision, additional characteriza-

tion of loads and environments, improvement of analytical model accuracy, and improved characterization of material behavior are among the options for controlling risk that can be quantitatively evaluated by probabilistic sensitivity analyses. Using results of probability sensitivity analysis, test and analysis programs focused on acquiring information about the most important risk drivers can be defined, thereby enabling limited financial resources to be allocated more effectively to control failure risk.

Probabilistic failure risk assessment can be employed in the design, development, and design verification processes to avoid the compounding of conservatism and margins that unnecessarily increase cost or weight. Probabilistic analysis is of particular value in design definition and verification when uncertainties exist about important governing parameters or when design conservatism and redundancy used in the past must be reduced to meet more stringent cost, weight, or performance requirements.

A general approach to probabilistic failure risk assessment and an application of the approach to fatigue crack growth in a heat exchanger tube are presented in the following.

2 PROBABILISTIC FAILURE RISK ASSESSMENT

Information from experience can be combined with information from analytical modeling to estimate failure risk quantitatively using the approach shown in Figure 1. This approach is applied individually to those failure modes identified for analysis. Probabilistic failure modeling is based on available knowledge of the failure phenomenon and of such governing parameters as loads and material properties, and it provides the prior failure risk distribution of Figures 1 and 2. This prior distribution can be modified to reflect available success/failure data in a Bayesian statistical analysis. The probabilistic failure risk assessment approach shown in Figures 1 and 2 is discussed in detail by Moore, et al. (Dec., 1992; Nov., 1992; June., 1992; and 1990).

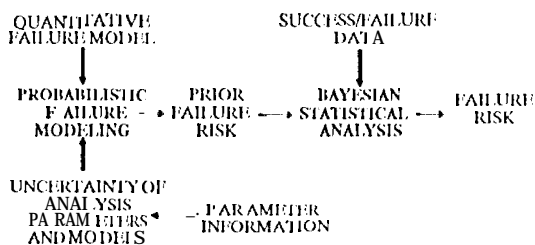


Fig. 1 Probabilistic failure risk assessment

Experience can include physical parameter information in addition to success/failure data. Information about physical parameters can be derived from measurements taken during tests or service, from analyses to bound or characterize parameter values, from applicable experience with similar systems, or from laboratory tests. Measurements of physical parameters used in analytical modeling, e.g., temperatures and loads, can be an important information source in failure risk assessment. Physical parameter information is incorporated into probabilistic failure modeling and is reflected in the prior failure risk distribution.

Success/failure data can be acquired from testing or service experience. The failure risk distribution resulting from the combination of the prior distribution and the success/failure data is the description of failure risk which is warranted by the information available. As additional information regarding governing physical parameters becomes available it can be incorporated into

analytical modeling to obtain a revised prior failure risk distribution. Additional information in the form of success/failure data can be processed by the Bayesian statistical analysis of Figure 1 to update the prior failure risk distribution using the procedure given by Moore, et al. (June, 1992 and 1990).

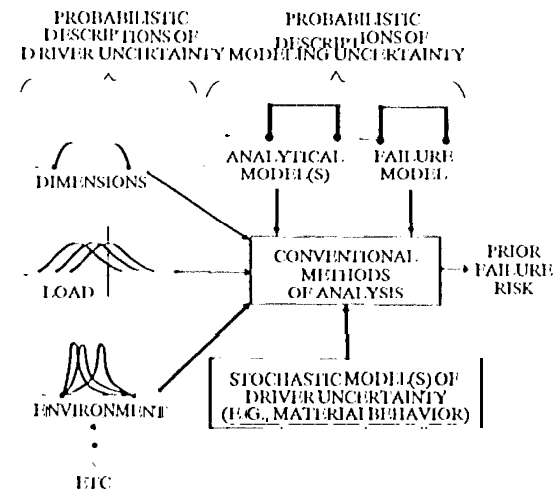


Fig. 2 Probabilistic failure modeling

The analysis procedures used in probabilistic failure modeling, shown in Figure 2, are directly derived from deterministic methods for analyses of failure modes which express failure parameters, such as burst pressure or fatigue life, as a function of governing parameters or drivers. For fatigue failure modes, the drivers include dimensions, loads, material behavior, model accuracy, and environmental parameters such as local temperatures. The accuracy of the models and procedures used in probabilistic failure modeling should be probabilistically described and treated as a driver. Probabilistic descriptions of model accuracy are based on experience in using the models and procedures, and when available, on tests conducted specifically to evaluate their accuracy.

A driver for which uncertainty is to be considered must be characterized by a probability distribution over the range of values it can assume. That distribution expresses uncertainty regarding specific driver values within the range of possible values. A driver probability distribution must represent both intrinsic variability of the driver and uncertain knowledge or limited information on which to base the driver characterization.

Stochastic drivers are characterized by using the information that exists at the time of analysis. If driver information is sparse, the probabilistic characterization of such a driver must reflect that sparseness. If extensive experimental measurements have been performed for a driver, its nominal value and characterization of its variability can be inferred directly from empirical data. However, if little or no directly applicable empirical data is available, analysis to characterize a driver or experience with similar or related systems must be used. Driver distributions must not overstate the precision implied by the available information.

Some general guidelines for characterizing stochastic drivers have emerged from case studies conducted to date, as given in Moore, et al. (Nov., 1992 and June., 1992). For drivers which have physical bounds, such as controlled dimensions or loads with physical upper limits, the Beta distribution parameterized with location, shape, anti scale parameters has been successfully used. If only bounds are known, a Uniform distribution is appropriate. For a driver whose variation can be thought of as due to the combined influence of a large number of small independent effects, the Normal distribution can be used. Past experience in characterizing a particular driver such as a material property may suggest the use of a particular distribution, for example, Weibull, Normal, or Lognormal.

A hyperparametric structure for driver distributions has been found useful in describing available information about a driver. For example, to characterize inner wall temperature uncertainty for the heat exchanger tube, information from engineering analysis was used to establish upper and lower bounds for the mean temperature. In order to capture the fact that the mean value of temperature was not known with certainty, the mean value was represented by a Uniform distribution between the upper and lower bounds. This Uniform distribution is the hyperdistribution associated with the mean temperature uncertainty, and its parameters are the associated hyperparameters.

Monte Carlo simulation has been used as the principal computational method in probabilistic failure modeling because it is a general method that can be used with failure models of any complexity. Continually increasing computer power due to improving hardware and software is steadily expanding the practical

application of Monte Carlo simulation. Efficient Monte Carlo techniques can be used to reduce the number of simulation trials when computational time is an issue. Certain analysis methods such as finite-element structural models, may be too computationally intensive for practical use in Monte Carlo simulation. However, the output of these models can be represented as response surfaces over the range of variation of significant parameters, see Moore, et al. (Dec., 1992). The uncertainties of response surface representations must be treated as drivers if significant.

Alternative computational methods, for example, FORM/SORM, see Madsen, et al. (1986), may fail to give accurate results for problems in which significantly nonlinear models are employed and driver uncertainty is large. Computational methods are discussed further by Moore, et al. (1990).

3. PROBABILISTIC CRACK GROWTH MODELING

In the crack growth analysis presented here, the life of a structure with initial flaws which is subjected to cyclic loading is computed probabilistically. The crack growth model used in this analysis can consider loads due to vibration, temperature gradient, and pressure. A Monte Carlo simulation procedure, shown in Figure 3, was used to calculate a life distribution.

A deterministic crack growth failure model is embedded within the simulation structure. The failure model expresses crack growth life as a function of drivers which may be either deterministic or stochastic. The drivers consist

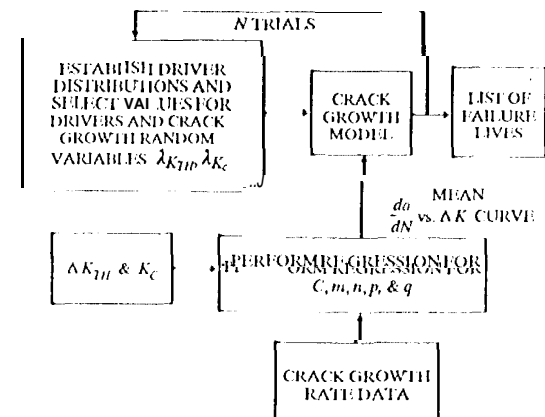


Fig. 3 Crack growth failure simulation

of geometry, loads, environmental parameters, material properties, and accuracy factors which account for uncertainties in the crack growth analysis.

The generalized Forman model, NASA/JSC (1986), was chosen as the basis for the stochastic crack growth rate model. The Forman equation is

$$\frac{da}{dN} = \frac{C(1-R)^m \Delta K^n [AK - \Delta K_{TH}]^p}{[(1-R)K_C - AK]^q} \quad (1)$$

in which da/dN is the crack growth rate, ΔK is the stress intensity factor range, ΔK_{TH} is the threshold stress intensity factor range, K_C is the critical stress intensity factor, R is the stress ratio, and C , n , m , p , and q are the model parameters. The generalized Forman equation captures the crack growth behavior in all of the growth rate regimes, and it can be extended to a stochastic crack growth rate model.

Fatigue crack growth rate data above 10^{-6} mm/cycle and below 10^{-2} mm/cycle do not exhibit a large amount of life variation. This can be seen by examining the extensive data sets of Virkler, et al. (1979) and Ghonem, et al. (1987) in which, for the same initial crack size, the ratio between the shortest and longest life is typically much less than two. This variation in the mid-rate region is small compared to the life variation that may occur due to uncertainty in other parameters such as ΔK_{TH} , stresses, initial crack geometry, etc. Many empirical da/dN vs. ΔK plots found in the literature seem to suggest that crack growth rate data scatter is large, but the apparently large scatter is an artifact of data gathering and data reduction. By comparing the low variability in lives to the much higher scatter in growth rates derived for the same data in Virkler, et al. (1979) and Ghonem, et al. (1987) it may be seen that localized growth rate scatter is not significant. The generalized Forman model can be easily employed to model variability of crack growth rate in the mid-rate region by stochastically varying C in Equation 1, although for the reasons outlined above it was deemed unnecessary.

In contrast to the crack growth in the mid-rate region, uncertainty in the high- and low-growth rate regions can be significant due to both intrinsic growth rate variability and lack of information in these regions. This uncer-

tainty may be represented in terms of the values of ΔK_{TH} and K_C which are asymptotes to the crack growth rate curve at its lower and upper ends, respectively. Uncertainty about these asymptotes is readily captured by using two stochastic scale parameters $\lambda_{K_{TH}}$ and λ_{K_C} . $\lambda_{K_{TH}}$ modifies the nominal value of the lower asymptote ΔK_{TH} and λ_{K_C} shifts the upper asymptote $(1-R)K_C$. Thus, the stochastic crack growth rate equation is given by

$$\frac{da}{dN} = \frac{C(1-R)^m \Delta K^n [AK - \lambda_{K_{TH}} \Delta K_{TH}]^p}{[(1-R)\lambda_{K_C} K_C - AK]^q} \quad (2)$$

The uncertainty in $\lambda_{K_{TH}}$ and λ_{K_C} may be characterized by probability distributions, or they may be treated parametrically as was done in the analyses presented here. Figure 4 shows the effect of perturbing $\lambda_{K_{TH}}$ and λ_{K_C} in the growth rate equation 2.

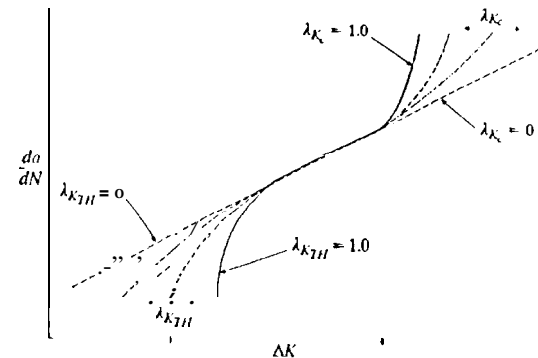


Fig. 4 Description of the stochastic crack growth equation in log-log space

As shown in Figure 3, the mean crack growth rate equation, which is an input to the crack growth model, is typically determined by performing a regression on crack growth data. The parameters C , m , n , p , and q are estimated by a least squares fit of the growth rate Equation 1. If the data is uncertain due to sparseness of data, or if the material test conditions do not closely represent the component operating environment, some of the other equation parameters may also be modeled stochastically. For example, if crack growth rate data were to be only available for a single stress ratio R , the uncertainty in m could be captured by describing m stochastically, based on values observed for similar materials.

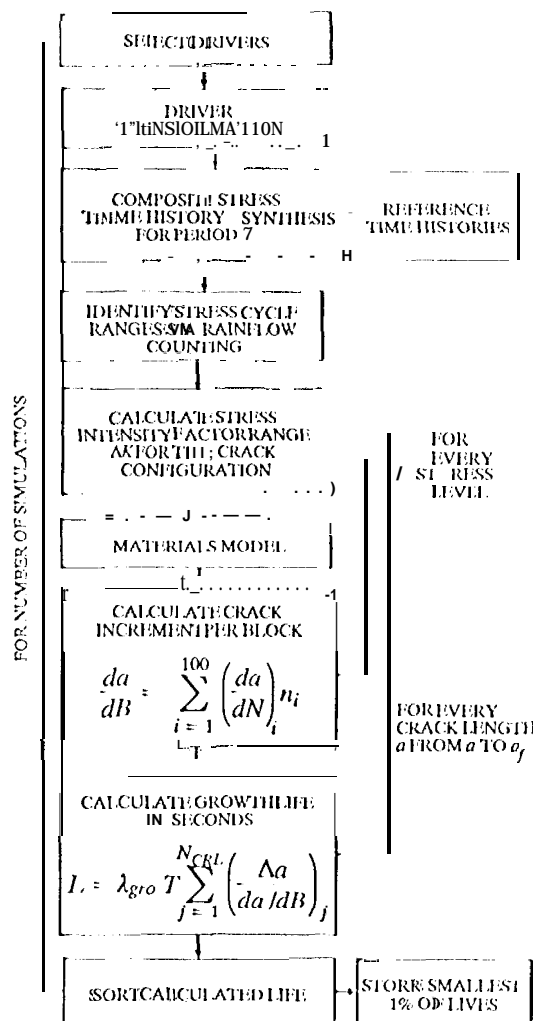


Fig. 5 Flowchart for crack growth calculation
4 CRACK GROWTH CALCULATIONS

The procedure used for calculating crack growth is shown in Figure 5. In the heat exchanger tube, vibration loads are primarily responsible for crack growth which can result in structural failure. The vibration environment was represented by power spectral density (1/s¹) envelopes.

The analyses of loads and stresses for the heat exchanger tube, and the crack growth calculations are described in detail by Moore, et al. (Dec., 1992 and June, 1992) and summarized by Sutharshana, et al. (1991). A stress history due to dynamic load sources was synthesized from the PSD envelopes. The stress cycles were obtained by performing a cycle

count on the synthesized stress time history using the rainflow cycle counting method. The load interaction in growth calculations was accounted for by using the generalized Willenborg retardation model, see Gallager (1974).

Since the traditional cycle-by-cycle crack growth life calculation is computationally intensive, an extremely fast yet accurate block-by-block approach first introduced by Brussat (1974) was used. In the block approach, a block growth rate da/dB is calculated at distinct crack lengths, starting from the initial crack length a_i to the final length a_f , by summing the crack growth rates da/dN from Equation 2 that correspond to ΔK_{eff} and R_{eff} for each stress level in the load block, as follows:

$$\frac{da}{dB} = \sum_{i=1}^{100} \left(\frac{da}{dN} \right)_i n_i \quad (3)$$

in which n_i is the number of cycles at the i th stress level. The life is computed by numerically integrating the inverted rate, per block between the initial and final crack length. The life in seconds is

$$L = \lambda_{gro} \tau \int_{a_i}^{a_f} \frac{da}{da/dB} \quad (4)$$

in which λ_{gro} is the uncertainty in the growth calculation and τ is the length of a load block in seconds. This calculation is performed as a summation over unequally divided N_{CRL} crack lengths, as follows:

$$L = \lambda_{gro} \tau \sum_{j=1}^{N_{CRL}} \left(\frac{\Lambda a}{da/dB} \right)_j \quad (5)$$

The standard stress intensity factor solution for a semi-elliptic crack in a finite width plate subject to axial and bending stresses was employed to calculate ΔK for the heat exchanger tube. The temperature difference across the wall of the tube (cold inside and hot outside) induces significant thermal stresses over the thickness, whose variation across tube thickness is similar to that of bending stresses. Standard stress intensity factor solutions for

cylinders with radial cracks, subjected to bending stresses over the thickness, are not available. The SIF expressions used in this analysis are given in NASA/JSC (1986).

(crack growth rate data from Rocketdyne (1989) were available for the heat exchanger tube material at stress ratios off{ = 0.16, 0.7, and 0.9. This crack growth data set was employed to derive the parameters of the stochastic Forman model given above.

5 DESCRIPTION OF DRIVERS

From among the load, dimension, and environment parameters that appear in the crack growth analysis for the heat exchanger tube, nineteen parameters were described probabilistically. Five of these parameters account for analysis model accuracy. These parameters, i.e., drivers, and their probability distributions are given in Table 1.

The initial crack shape aspect ratio a/c was represented by a Uniform distribution with end points of 0.2 and 1.0. The crack geometry was then defined by treating initial crack length a_i parametrically. Life was simulated with the value of a_i fixed at 0.025 mm, 0.063 mm, 0.13 mm, and 0.19111111. The crack shape distribution was based on an assessment of the crack aspect ratios that could result from tile heat exchanger manufacturing process.

The heat exchanger tube wall thickness is nominally 0.312 mm, which leads to the concern that "short crack" behavior may be relevant. Short crack growth rate curves have been observed by Morris, et al. (1983) not to have definite thresholds. If a threshold exists, it is a conservative assumption for the linear segment of the curve in the mid-rate region to be extrapolated down into the threshold region. Fixing $\lambda_{K_{TH}} = 0$ in the stochastic Forman equation accomplishes this, as shown in Figure 4. Analyses were performed with values of $\lambda_{K_{TH}}$ at 0.0, 0.1, 0.2, etc., to study the impact of tile threshold location. Since growth is in the low rate region, the driver λ_{K_C} is not relevant, and its value was fixed at unity.

The stress intensity factor calculation accuracy factor λ_{SIF} accounts for the C1101 in tile standard stress intensity factor solution and the uncertainty associated with employing a finite width plate solution for a crack in a

Table 1. Description of drivers used in the heat exchanger tube analysis

DRIVER	DISTRIBUTION	RANGE
Initial crack size a_i , mm	Fixed	0.025 to 0.19
Initial crack shape a/c	Uniform	.2 to 1.0
Threshold stress intensity factor range accuracy factor $\lambda_{K_{TH}}$	Uniform	0.0 to 1.0
Fracture toughness accuracy factor λ_{K_C}	Fixed	0.0 to 1.0
Random load adjustment factor λ_{RANDOM}	$\left\{ \begin{array}{l} \text{Normal } (\mu, \sigma^2) \\ \mu = 0.77 \\ \sigma = 0.12 \end{array} \right\}$	-
Sinusoidal load adjustment factor $\lambda_{SINUSOIDAL}$	$\left\{ \begin{array}{l} \text{Normal } (\mu, \sigma^2) \\ \mu = 0.71 \\ \sigma = 0.14 \end{array} \right\}$	-
Aerodynamic load factor $\lambda_{AERODYN}$	Uniform	.5 to 1.5
Aerostatic load factor $\lambda_{AEROSTAT}$	Uniform	.8 to 1.2
Inner wall temperature T_i (°K)	$\left\{ \begin{array}{l} \text{Normal } (\mu, \sigma^2) \\ \mu \sim \text{Uniform } (270, 370) \\ \sigma \sim \text{Uniform } (16.1, 31.4) \end{array} \right\}$	-
Outer wall temperature T_o (°K)	$\left\{ \begin{array}{l} \text{Normal } (\mu, \sigma^2) \\ \mu \sim \text{Uniform } (444, 505) \\ \sigma \sim \text{Uniform } (26.7, 27.5) \end{array} \right\}$	-
Internal pressure p_i , MPa	$\left\{ \begin{array}{l} \text{Normal } (\mu, \sigma^2) \\ \mu \sim U(26.3, 28.8) \\ \sigma = 0.476 \end{array} \right\}$	-
Inner diameter D_i , mm	$\left\{ \begin{array}{l} \text{Beta } (\rho, \theta) \\ \theta = \text{Uniform } (.5, 20) \end{array} \right\}$	4.79 to 4.86
Wall thickness t , mm	$\left\{ \begin{array}{l} \text{Beta } (\rho, \theta) \\ \rho = .27 \\ \theta = \text{Uniform } (.5, 20) \end{array} \right\}$	0.2910 to 0.40
Dynamic stress analysis accuracy factor λ_{DYN}	Uniform	.8 to 1.2
Static stress analysis accuracy factor λ_{STAT}	Uniform	.9 to 1.1
Stress intensity factor calculation accuracy factor λ_{SIF}	Uniform	.9 to 1.1
Growth Calculation accuracy factor λ_{GRO}	Uniform	ln .2 to ln 1.75
Neuber's rule accuracy factor λ_{NEU}	Uniform	.6 to 1.4
Weld coefficient stress concentration accuracy factor λ_{CFI}	Uniform	.8 to 1.2

cylinder. A Uniform distribution was used for λ_{SIF} with a range of 0.9 to 1.1. The growth

calculation accuracy factor λ_{gro} accounts for uncertainties in the block-by-block growth calculation and in transformation of a variable amplitude stress history to a constant amplitude stress vs. number of cycles table using rainflow counting. Evidence in the literature indicates that factors of two between the calculated crack growth life and tests are appropriate. Since crack propagation is the result of a number of multiplicative events, the distribution on λ_{gro} was specified in log space. A Uniform distribution was used with the lower bound set at $\ln(1/2)$. In order for the mean value to lag, to be 1.0, the upper bound was set at $\ln(1.75)$.

The Beta distributions characterizing heat exchanger tube dimensions in Table 1 are parameterized by location, scale, and range parameters which are given as μ , θ , and the end points of the range, respectively.

61-U, SIM 1S

Figure 6 presents the left-hand tail of the simulated failure distribution for the heat exchanger tube. The ordinate of these graphs is the failure probability. The abscissa is the life in seconds for crack growth through the thickness of the heat exchanger tube. Figure 7 illustrates the effects of the crack growth threshold and initial crack size on life at a (0.001 failure probability.

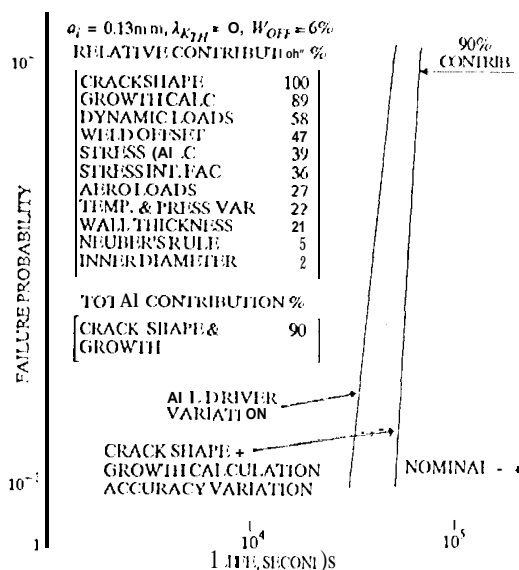


Fig. 6 Life distributions and driver sensitivities

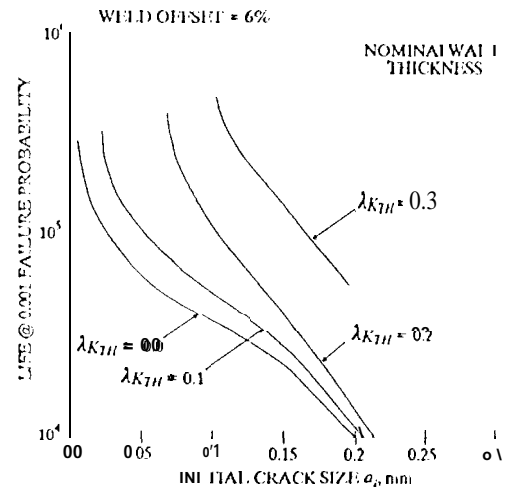


Fig. 7 Crack size and growth threshold effects

The results in Figure 6 are given for an initial crack size $a_i = 0.13 \text{ mm}$, $\lambda_{KTH} = 0.1$. The left curve labeled "all driver variation" is for a simulation where all the drivers were allowed to vary except a_i , λ_{KTH} , and λ_{KC} . The "nominal" value shown on the graph is for an analysis with all the drivers fixed at nominal values. Measures of the relative importance of individual drivers are given in the upper left corner in Figure 6. These were obtained by finding marginal effects of driver uncertainties using several sensitivity runs, where one driver was allowed to vary while the rest were held at nominal values. The crack shape and the growth calculation accuracy are the most important drivers with a 90% contribution to decrease in life. The right-hand curve in Figure 6 shows the shift to the left due to the variation in the crack shape and growth calculation accuracy.

7 CONCLUSIONS

For this heat exchanger tube application, the uncertainty due to incomplete knowledge and limited information concerning the accurate characterization of analysis models and physical driver parameters have a much larger impact on failure risk than do any intrinsic parameter variability. The information available was insufficient to meaningfully characterize initial crack size and threshold stress intensity factor for "short cracks". Consequently these important drivers were treated

parametrically in order to show their impact on crack growth life and to better define information that is needed to reduce failure risk. A tradeoff between knowledge of initial crack size, and knowledge of short crack threshold stress intensity factor, conditioned on the uncertainties in other drivers, can be inferred from the results shown in Figure 7. For a conservative "short crack" threshold ($\Delta K_{TH} = 0$) assumption, inspection techniques that can detect 0.13mm initial cracks with high reliability are required to achieve a life of about 3×10^4 seconds at 0.001 failure probability. On the other hand, if more representative crack growth data can be generated that can reliably establish a nonzero growth threshold ($\Delta K_{TH} > 0$), then the requirements on the inspection may be relaxed while achieving the same life at 0.001 failure probability.

ACKNOWLEDGMENTS

The research described in this publication was carried out by the Jet Propulsion Laboratory, (California Institute of Technology, under a contract with the National Aeronautics and Space Administration. The authors gratefully acknowledge the technical contributions made by engineering personnel of Rocketdyne Division, Rockwell International, Inc., Canoga Park, CA, USA.

REFERENCES

- Brussat, P.J., 1974, "Rapid Calculation of Fatigue Crack Growth by Integration," Fracture Toughness and Slow Stable Cracking, ASTM STP 559, American Society for Testing and Materials, pp. 298-311.
- Gallagher, J.P., and Hughes, P.S., 1974, "Influence of the Yield Stress on the Overload Affected Fatigue Crack Growth Behavior of 4340 Steel," AFFDL-74-27, Air Force Flight Dynamics Laboratory, Wright-Patterson Air Force Base, Ohio.
- Ghoniem, H., and Dore, S., 1987, "Experimental Study of the Constant-Probability Crack Growth Curves Under Constant Amplitude Loading," Engineering Fracture Mechanics, vol. 27, No.1, pp.1 - 25.
- Madsen, H.O., Krenk, S., and Lind, N.C., 1986, Methods of Structural Safety, Prentice-Hall, Englewood Cliffs, New Jersey.
- Moore, N., et al., Dec. 1992, An Improved Approach for Flight Readiness Certification - Probabilistic Models for Flaw Propagation and Turbine Blade Fatigue Failure, Volume 1, JPL Pub. 92-32, Jet Propulsion Laboratory, California Institute of Technology, Pasadena.
- Moore, N., Ibbeler, D., and Creager, M., Nov. 1992, "Probabilistic Service Life Assessment," Reliability Technology - 1992, AD-Vol. 2.8, American Society of Mechanical Engineers, ISBN 0-7918-1095-X.
- Moore, N., et al., June 1992, An Improved Approach for Flight Readiness Certification - Methodology for Failure Risk Assessment and Application Examples, Volume 1, JPL Pub. 92-15, Jet Propulsion Laboratory, California Institute of Technology, Pasadena.
- Moore, N., Ibbeler, D., and Creager, M., 1990, "A Methodology for Probabilistic Prediction of Structural Failures of Launch Vehicle Propulsion Systems," Paper No. 90-1140-CP, Proceedings of the AIAA 31st Annual Structures, Structural Dynamics and Materials Conference, pp. 1092-1104.
- Morris, W.J., and James, M.J., 1983, "Investigation of the Growth Threshold for Short Cracks," Proceedings of the International Symposium on Fatigue Crack Growth Threshold Concepts, AIME, pp. 479-495.
- NASA/JSC 27287, 1986, Fatigue Crack Growth Computer Program, "NASA/FLAGRO" Manual, National Aeronautic and Space Administration, Johnson Space Center, Houston, TX.
- Rocketdyne Division, 1989, "Fatigue Crack Growth Rate Testing of Welded 316L," Rockwell International, Canoga Park, California.
- Sutharshana, S., et al., 1991, "A Probabilistic Fracture Mechanics Approach for Structural Reliability Assessment of Space Flight Systems," Advances in Fatigue Lifetime Predictive Techniques, Special Technical Publication 112.2, American Society for Testing and Materials.
- Virkler, D. A., Hillberry, B. M., and Goel, P. K., 1979, "Statistical Nature of Fatigue Crack Propagation," Journal of Engineering Materials and Technology, ASME, Vol. 101, April, pp. 148-153.